

Modelling the anisotropic damage behaviour of highly-filled particulate composites via a multi-scale “morphological approach”

S. Darbois¹, C. Nadot-Martin¹, D. Halm¹, M. Gueguen¹, A. Dragon¹, A. Fanget²
¹Laboratoire de Mécanique et de Physique des Matériaux (UMR CNRS n°6617),
Ecole Nationale Supérieure de Mécanique et d'Aérotechnique, Futuroscope-
Chasseneuil Cedex, France; ²Centre d'Etudes de Gramat, Gramat, France.

1. Introduction

This paper outlines a non-conventional modelling approach, called morphological approach (MA), specifically addressed to highly-filled particulate composites in which damage consists in grain / matrix debonding. Some energetic composites, notably propellant-like materials and high explosives, could be concerned as studied with regard to their vulnerability.

The MA stands as a *direct* scale transition approach whether material and / or geometrical non-linearities are at stake. This feature makes it relevant to deal with damage. First, the MA starts by a *direct* geometrical schematization of the real initial microstructure in which each grain and matrix intergranular zone are explicitly represented (with no mesh). Moreover as shown for example in [1] for sound materials, the MA does not require any prior linearization of local non linear constitutive laws contrarily to homogenization schemes referring to the notion of equivalent linear composite, see [2] for a review of existing linearization procedures and their possible influence on the global estimates. The MA solving procedure for sound viscoelastic composites [3,1,4] regards directly the time-domain without using the Laplace-Carson transform (see also [5]). At last, the MA allows to access to local field estimates with fluctuations in the matrix governed by local morphology. This feature is essential for the description of interfacial damage.

In fact, the origin of the above advantages lies in the coupling between the aforementioned *explicit* geometrical schematization and a simplified kinematical description (assumptions regarding the displacement field). Those two ingredients have been initially proposed by [6] for sound, elastic ‘bonded granulates’. The non-linear developments mentioned above for sound materials have proved the efficiency of these two very bases. In particular, the relevance of the kinematical description has been appreciated through comparisons of local and global estimates with FE calculations for specific periodic hyperelastic and viscohyperlastic composites [1] and random ones [7].

The specific contribution of the present work lies in exemplifying how the progressive microstructural damage events, i.e. formation and closure of interfacial defects on the grain / matrix contacts, is being followed in the framework of the MA, small strain version. Sec. 2 recalls the theoretical background detailed in [8] of the MA in the presence of interfacial damage with no ingredient to trace its evolution. The principal ingredients of the MA (schematization of the microstructure, different stages of the solving procedure for a fixed number of open and closed defects) are first recalled. Then, analytical results obtained at both scales for linear elastic constituents (grains and matrix) are briefly presented as an illustration of the effects captured by the MA. The ingredients necessary to describe damage evolution are given in Sec. 3, where the

nucleation and closure criteria for the defects are summarized. Sec. 4 gives a numerical illustration of the ability of the MA to deal with damage evolution in a random three-dimensional composite containing 400 grains submitted to a complex loading path. The homogenized response is discussed with special attention paid on the evolution of the damage induced anisotropy as a function of the chronology of local damage events (discrete sequence of nucleations and closures). The ability of the MA to give access to the position and morphology of interfacial defects, is illustrated through 3D representations of the damaged microstructure.

2. Morphological approach in presence of damage (fixed state) by [8]

2.1. Direct geometrical schematization of the initial microstructure

The random microstructure of a highly filled particulate composite is represented by an aggregate of polyhedral grains interconnected by thin matrix layers with constant thicknesses. This schematization is illustrated in Fig. 1. For each layer α , four “morphological parameters” are identified in the initial configuration, [6]:

- h^α , the constant thickness of layer α
- A^α , the projected area of layer α , the associated volume is then $A^\alpha h^\alpha$
- d^α , the vector linking the centroids of the polyhedra separated by layer α
- n^α , the unit vector normal to the plane interface grain/layer α .

Once the grains are approximated by polyhedra (satisfying the condition of parallelism between the interfaces of opposite grains), the parameters d^α , n^α and h^α are readily identified. The projected area A^α – leading to the definition of the matrix zone between two neighboring grains called “layer α ” – is identified as follows. Starting from the centroids of the two grains, the two opposite interfaces are projected on the middle plane of the intergranular zone. Then, an average projection is defined and chosen as the area A^α . In this way, layer α (associated volume $A^\alpha h^\alpha$) does not correspond exactly to the matrix zone strictly confined between the two opposite interfaces. It can be larger as illustrated in Fig. 1c (2D representation).

Practically, the challenge is to optimize the polyhedrization process, namely the correspondence of the “true” microstructure with the schematized one, in order to confer a fair relevance on the morphological parameters. X-ray tomography together with available tools of morphological analysis of 3D images may be used to this aim.

One may emphasize the direct and explicit character of such a schematization since each grain and each matrix intergranular zone are represented in relationship to the real material morphology. This feature differentiates the MA notably from the Eshelby-based self-consistent-like estimates.

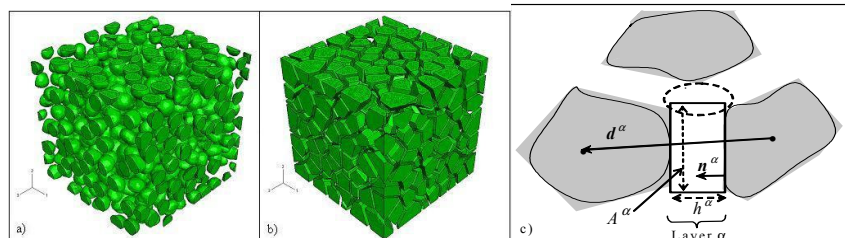


Fig. 1. Illustration of the geometrical schematization: a) real microstructure (X-ray tomography), b) schematized microstructure, c) morphological parameters for a layer α , [6].

2.2. Localization-homogenization problem: principal tools and stages of the solving procedure

The second set of starting hypotheses of the MA consists in simplifying kinematical assumptions regarding the local displacement field in the schematized volume. They are recalled below within the linearized deformation (small strain) framework, [6]. The grain centroids are displaced so as to conform to a global, homogeneous displacement gradient \mathbf{F} (data for the local problem). The grains themselves are supposed homogeneously deformed and the corresponding displacement gradient \mathbf{f}^0 assumed to be common to all grains of the schematized volume. Each interconnecting layer is subjected to a homogeneous deformation, proper to the layer α under consideration and noted \mathbf{f}^α . Local disturbances at grain edges and corners (see circled zone in Fig. 1c) are neglected on the basis of thinness of the layers.

The interfacial defects and relative displacement jumps have been incorporated by [8] in a compatible way with this kinematical description. It is proved that the displacement discontinuity vectors across debonded interfaces are necessarily affine functions of the spatial coordinates. This means that the simplified (piecewise linear) kinematics proper to the MA does not allow accounting for partial decohesion of grain/matrix interfaces: there is either decohesion almost everywhere, or there is no decohesion. Moreover, the second hypothesis regarding \mathbf{f}^0 as common to all grains, imposes only two possible configurations for a layer α : either no decohesion, or simultaneous decohesion of its both interfaces. In order to make acceptable this double decohesion (if any), a supplementary constraint to the geometrical schematization has been added by [8]: any two opposite interfaces must have close geometrical properties (shape and area). Furthermore and considering the parallelism of opposite interfaces in course of deformation, the authors consider that the mean displacement discontinuity vectors across the interfaces of a debonded layer α are opposite.

By taking into account conditions of displacement jump (with affine form for the jumps $b_i^\alpha = f_{ij}^{\alpha D} y_j$, see [8] for details), the displacement gradient \mathbf{f}^α for a debonded layer α (i.e. with defects at its interfaces), is given by Eq. (1)₁. For a layer α whose both interfaces are cohesive \mathbf{f}^α is obtained by using the continuity of displacements on the grain/layer interfaces (see Eq. (1)₂):

$$f_{ij}^\alpha = \begin{cases} f_{ij}^0 + (F_{ik} - f_{ik}^0) a_k^\alpha n_j^\alpha / h^\alpha + f_{ij}^{\alpha D} & \text{if the layer } \alpha \text{ is debonded} \\ f_{ij}^0 + (F_{ik} - f_{ik}^0) a_k^\alpha n_j^\alpha / h^\alpha & \text{if not} \end{cases} \quad (1)$$

The supplementary term $\mathbf{f}^{\alpha D}$ in Eq. (1)₁ represents the specific contribution of two interfacial defects located at the interfaces of the debonded layer α considered. If the material is sound, \mathbf{f}^α is obviously given by Eq. (1)₂ for every layer α .

The MA morphology and kinematics framework in the presence of damage allows taking into account some strain heterogeneity in the matrix seen as an assembly of layers with different geometrical characteristics. This heterogeneity is not only governed by local morphology but also by local damage events (see the dependence of \mathbf{f}^α on the morphological parameters proper to the layer α considered and on $\mathbf{f}^{\alpha D}$ for debonded layers). This is a positive feature in the context of non linear homogenization since local heterogeneity has to be taken into account to ensure a fair estimate of the global behaviour, (see e.g. [9]).

The compatibility between local motion defined above and the global one characterized by the given displacement gradient \mathbf{F} (i.e. $\mathbf{F} = \langle \mathbf{f} \rangle_V +$ contribution of defects) is ensured through a geometrical condition to be satisfied by the morphological parameters of the schematized material, see [8] for detailed form and interpretation.

For a given number of open and/or closed defects, the grains displacement gradient \mathbf{f}^g is deduced from the use of the generalized Hill lemma, by employing the local constitutive laws for the grains and the matrix and using the hypothesis of no sliding, i.e. infinite friction coefficient presumed on closed defect lips (see Sec. 3 in [8] for details). Then, the knowledge of \mathbf{f}^g allows the backwards calculation of the composite response at both scales: \mathbf{f}^α for any layer α by using Eq. (1), local strains and associated stresses by the local constitutive laws and finally the homogenized stress tensor by volume averaging of the local one.

The foregoing solving procedure remains valid whatever are the constituents' constitutive laws. This procedure is analytical in the small strain framework. At this stage, it is nevertheless partial. Indeed, since nothing has been formulated regarding the detailed expression of the displacement jumps in function of macroscopic displacement gradient \mathbf{F} (except their linearity with respect to local spatial coordinates due to the kinematical description), the local fields and homogenized stress will be expressed in function of the set $\{\mathbf{f}^{ad}\}$, more precisely the set of their symmetric part. This offers an advantage to identify in an explicit way the contributions of defects in the expressions obtained at both scales (see Eq. (6) in Subsec. 2.3 for an illustration). Evidently, a complementary stage, depending on the local behaviour of constituents, is required to explicit some of the damage-induced local quantities. In Subsec. 2.3 are summarized the basic results obtained for isotropic linear-elastic constituents (grains and matrix). Within this framework, a complementary localization-homogenization approach has been put forward.

2.3. Results in elasticity and complementary localization-homogenization approach

In the case of isotropic linear-elastic constituents (grains and matrix), the analytical expressions of the local strain field and of the homogenized Cauchy stress tensor, resulting from the first stage of the scale transition according to the methodology summarized above, depend on the following quantities in addition to the elastic moduli of constituents:

$$\text{Global strain } \mathbf{E} = \text{Sym. } \mathbf{F} \quad (2)$$

Damage-induced strains:

$$\{\boldsymbol{\epsilon}^{\beta D}; \beta \in L^{open}\}, \quad \{\boldsymbol{\epsilon}^{fD}; f \in L^{closed}\}, \quad (3)$$

Initial morphological tensorial parameter:

$$\bar{T}_{ijkl} = \frac{1}{V} \sum_{\alpha} d_i^{\alpha} n_j^{\alpha} d_k^{\alpha} n_l^{\alpha} A^{\alpha} / h^{\alpha}, \quad (4)$$

Damage tensorial parameters:

$$D_{ij} = \frac{1}{V} \sum_{\beta \in L^{open}} d_i^{\beta} n_j^{\beta} A^{\beta}, \quad \bar{D}_{ijkl} = \frac{1}{V} \sum_{\beta \in L^{open}} d_i^{\beta} n_j^{\beta} d_k^{\beta} n_l^{\beta} A^{\beta} / h^{\beta}. \quad (5)$$

The strain of any layer α in the schematized volume, i.e. $\boldsymbol{\varepsilon}^\alpha = \text{Sym. } \mathbf{f}^\alpha$, is also function of its local morphological parameters according to Eq. (1).

In Eqs. (3) and (5), L^{open} , respectively L^{closed} , represents the set of layers with open, respectively closed, defects at their interfaces. In accordance with Eq. (1)₁, the strain $\boldsymbol{\varepsilon}^{\beta D} = \text{Sym. } \mathbf{f}^{\beta D}$, respectively $\boldsymbol{\varepsilon}^{fD} = \text{Sym. } \mathbf{f}^{fD}$, represents for a layer $\beta \in L^{open}$, respectively $f \in L^{closed}$, the contribution of open, respectively closed, defects at its own interfaces to the total strain of the layer. In Eq. (4), superscript α under the summation symbol denotes summation over all layers (debonded or not).

The estimates at both scales account for initial morphology and internal organization of grains inside the volume through the presence of the macroscopic fourth-order structural tensor $\bar{\mathbf{T}}$ given by Eq. (4). The reader may refer to [6] where it is shown that $\bar{\mathbf{T}}$ reflects possible material texture (initial anisotropy) and irregularities in grain shape and in layer thickness. Moreover, the two tensors \mathbf{D} and $\bar{\mathbf{D}}$ emerge naturally in the local and global estimates. They stand as macroscopic damage parameters testifying about degradation mechanism generated within the aggregate. Since no sliding has been considered for closed defects (infinite friction coefficient), these defects do not contribute to the degradation of the material (see the summations over layers $\beta \in L^{open}$ in Eq. (5)). Note also the morphology influence in the very nature of \mathbf{D} and $\bar{\mathbf{D}}$: these tensors account for the granular character of the microstructure through the vectors \mathbf{d}^β involved in their definition in addition to the defect normal vectors \mathbf{n}^β . The tensorial parameters \mathbf{D} and $\bar{\mathbf{D}}$ - in addition to the textural tensor $\bar{\mathbf{T}}$ related to initial morphology - allow to account, in a general 3D context, for coupling of primary anisotropy (if any) with the damage-induced one.

As an illustration, the form of the strain $\boldsymbol{\varepsilon}^\alpha$ for any layer α (debonded or not) is given below:

$$\boldsymbol{\varepsilon}^\alpha = \overbrace{\mathbf{C}^\alpha(\bar{\mathbf{T}}, \mathbf{D}, \bar{\mathbf{D}})}^{\boldsymbol{\varepsilon}^{\alpha(r)}} : \mathbf{E} + \boldsymbol{\varepsilon}^{\alpha(d)}(\{\boldsymbol{\varepsilon}^{\beta D}\}, \{\boldsymbol{\varepsilon}^{fD}\}; \bar{\mathbf{T}}, \mathbf{D}, \bar{\mathbf{D}}) + \begin{cases} \boldsymbol{\varepsilon}^{\alpha D} & \text{if layer } \alpha \text{ is debonded} \\ \emptyset & \text{if not} \end{cases} \quad (6)$$

Three contributions are put forward in Eq. (6), the two first ones depending on global parameters related to initial morphology ($\bar{\mathbf{T}}$) and damage configuration (\mathbf{D} and $\bar{\mathbf{D}}$) and on local morphology of the layer α considered: The first one, $\boldsymbol{\varepsilon}^{\alpha(r)}$, is reversible with respect to \mathbf{E} (with \mathbf{C}^α the corresponding strain localisation tensor degraded, via \mathbf{D} and $\bar{\mathbf{D}}$, by the presence of open defects inside the volume). The second one, $\boldsymbol{\varepsilon}^{\alpha(d)}$, involves the full set $\{\boldsymbol{\varepsilon}^{\beta D}\} \cup \{\boldsymbol{\varepsilon}^{fD}\}$ related to the effect of any kind of defects (open and closed) in the material. The last one, $\boldsymbol{\varepsilon}^{\alpha D}$, corresponds to the contribution of the defects (if any) at the interfaces of the considered layer α .

Due to infinite friction, $\boldsymbol{\varepsilon}^{fD}$, for a layer $f \in L^{closed}$ with closed defects at its interfaces, does not depend on the macroscopic strain \mathbf{E} since no sliding is allowed. As a result, the set $\{\boldsymbol{\varepsilon}^{fD}\}$ acquires the status of internal variables accounting for the distortion due to the blockage of closed defects inside the volume. On the contrary the opening of a defect naturally depends on \mathbf{E} and therefore the local induced strain $\boldsymbol{\varepsilon}^{\beta D}$ for any layer $\beta \in L^{open}$ as well. This is why the foregoing scale transition has been completed by a second stage –called complementary localization-homogenization procedure in [8] - in order to establish the explicit dependence of $\boldsymbol{\varepsilon}^{\beta D}$ on global strain \mathbf{E} . Using thermodynamics as a guide, the main advantage of the advanced approach is its possible generalization for time-dependent materials. In elasticity, the strain $\boldsymbol{\varepsilon}^{\beta D}$ induced in a layer β by the open defects at its own interfaces, is obtained as a function of \mathbf{E} , and local morphological features as follows:

$$\varepsilon_{ij}^{\beta D} = - Id_{ij\mu\nu} d_\nu^\beta n_m^\beta / h^\beta M(\bar{\mathbf{T}}, \mathbf{D}, \bar{\mathbf{D}})_{\mu\nu\kappa l} E_{lk} + r_{ij}^{\beta D} \quad (7)$$

The detailed form for $M(\bar{T}, \mathbf{D}, \bar{D})$ depending on elastic properties of constituents is given in [8]. Note that $\boldsymbol{\varepsilon}^{\beta D}$ is influenced (via \mathbf{M}) by global initial morphology and damage configuration. The constant tensor $\mathbf{r}^{\beta D}$ with respect to \mathbf{E} , represents a residual strain induced in the layer β by residual opening of the defects at its interfaces for $\mathbf{E} = \mathbf{0}$. Physically, such a residual opening is linked to the roughness of corresponding interfaces. With Eq. (7), local strain field and global response of the elastic damaged composite, are expressed in terms of global strain \mathbf{E} , distortion internal variables $\{\boldsymbol{\varepsilon}^{fD}\}$, residual opening strain-like quantities $\{\mathbf{r}^{\beta D}\}$, in addition to global parameters related to initial morphology (\bar{T}) and damage configuration (\mathbf{D} , \bar{D}). For example, the form of the homogenized stress becomes:

$$\boldsymbol{\Sigma} = \tilde{\mathbf{L}}(\bar{T}, \mathbf{D}, \bar{D}) : \mathbf{E} + \boldsymbol{\Sigma}^{(d)1}(\{\mathbf{r}^{\beta D}\}; \bar{T}, \mathbf{D}, \bar{D}) + \boldsymbol{\Sigma}^{(d)2}(\{\boldsymbol{\varepsilon}^{fD}\}; \bar{T}, \mathbf{D}, \bar{D}) \quad (8)$$

3. Damage state and configuration evolution, discrete modelling

Thanks to its explicit schematization of the real microstructure, notably of the grain/matrix interfaces, in addition to the accessibility to an estimate of local fields, the MA allows to treat damage evolution at the local scale (that of the constituents). Thus, instead of considering \mathbf{D} and \bar{D} as macroscopic damage internal variables and establishing evolution equations for these variables, the direct discrete modelling is put forward here considering the sequence of discrete interfacial local damage events. In such a strategy \mathbf{D} and \bar{D} remain as damage parameters reflecting current induced degradation and anisotropy in the local and global estimates as presented above.

Two criteria are to be formulated now. The first one concerns the nucleation of defects, and the second one is a closure criterion which allows describing the evolution of damage configuration (i.e. the respective proportion of open and closed defects for a given total number of defects). Practically, the both criteria will be tested for each increment of a simulated loading path. When a criterion is satisfied for one or several interfaces, the parameters \mathbf{D} and \bar{D} will be actualized in consequence (by adding or suppressing corresponding layers in the summations, see Eq. (5)).

3.1. Nucleation criterion

Following the hypothesis of no sliding ('infinite friction coefficient'), the nucleation is supposed to happen in a mode I way.

Consider a layer α with sound interfaces. The displacement field in this layer is noted \mathbf{u}^α , and it is noted \mathbf{u}^0 in the grains. Two particular points P_1 and P_2 are defined on each side of the first interface I_1^α , the one in the grain and the other in the matrix. Both points are equidistant from their normal projection B_1 on the interface, with B_1 the gravity center of I_1^α (see Fig. 2).

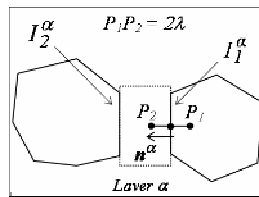


Fig. 2. Definition of testing points P_1 and P_2 .

The difference $\Delta\mathbf{u}=\mathbf{u}^\alpha(P_2)-\mathbf{u}^0(P_1)$ is expressed using the linearity of the fields \mathbf{u}^α and \mathbf{u}^0 (according to the kinematical assumptions, see Subsec. 2.2) and Eq. (1)₂ for \mathbf{f}^α . The knowledge of $\Delta\mathbf{u}$ allows to evaluate the normal projection of the difference of actual positions of P_1 and P_2 . It is then considered that when this distance, noted d_{norm}^α , reaches a certain critical value, decohesion happens at the interfaces of the layer α :

$$d_{norm}^\alpha = d_{critical} \Leftrightarrow \text{debonding} \quad , \quad d_{norm}^\alpha = 2\lambda + \Delta\mathbf{u} \cdot \mathbf{n}^\alpha \quad (9)$$

The expression of d_{norm}^α involved in the criterion shows that the nucleation of defects at the interfaces of any layer α is conditioned by the local morphology in the neighbourhood of the interfaces (via geometrical features of the layer α considered in $\Delta\mathbf{u}$) and by the orientation of the interfaces (via \mathbf{n}^α). Moreover the nucleation depends in the same way for all layers (via $\Delta\mathbf{u}$), on initial global morphology and on damage configuration if any other layer is already debonded in the volume (see [10] for detailed form of $\Delta\mathbf{u}$).

The value $d_{critical}$ is a sort of critical defect-incipience opening, depending on the material studied and linked to the adhesion properties of the matrix and the grains. The identification of $d_{critical}$ for a particular composite will depend on the characteristic length 2λ (distance chosen between two points P_1 and P_2 on each side of the interface).

Since decohesion is supposed to take place in a normal mode, a layer α for which Eq. (9) is satisfied becomes a layer of type β (namely with open defects at its interfaces). The summations involved in the definition of the damage parameters \mathbf{D} and \mathbf{D} are actualized by adding this new layer. The direct contribution of the defects to the total strain of the layer β is given by Eq. (7).

3.2. Closure criterion

The closure criterion is given in terms of local normal displacement jump in the following way for a layer β with open defects at its interfaces:

While $\langle \mathbf{b}^\beta \rangle_{I_1^\beta} \cdot \mathbf{n}^\beta > 0$ defects at the interfaces of the layer β are open,

When $\langle \mathbf{b}^\beta \rangle_{I_1^\beta} \cdot \mathbf{n}^\beta = 0$ defects at the interfaces of the layer β are closed.

The test of the closure criterion requires the calculation of the average displacement jump $\langle \mathbf{b}^\beta \rangle_{I_1^\beta}$ at each loading step following the nucleation of

defects at the interfaces of the layer β . Considering the affine form of the jump across the interface I_1^β , the latter is linked to $\mathbf{f}^{\beta D}$ via: $\langle \mathbf{b}^\beta \rangle_{I_1^\beta} = \mathbf{f}^{\beta D} \mathbf{y}^{B_I}$ with \mathbf{y}^{B_I}

the coordinates of B_I . The symmetric part of $\mathbf{f}^{\beta D}$, namely $\boldsymbol{\varepsilon}^{\beta D}$, is known via Eq. (7).

The determination of the rotation $\boldsymbol{\omega}^{\beta D} = \text{Antisym. } \mathbf{f}^{\beta D}$ makes use of a specific treatment whose only the principal stages are presented here, (see [10] for details).

It is supposed that the rotation axis of the layer β after debonding corresponds to the edge of the interface I_1^β for which the difference of displacement vectors of two points on each side of this edge is minimum just before nucleation of defects.

A local basis associated to the layer is thus defined and conserved further. The rotation tensor $\boldsymbol{\omega}^{\beta D}$ is calculated at each loading step using this basis and in such a way that the mean displacement jumps on both interfaces be opposite. By this

way, $\mathbf{f}^{\beta D}$ and therefore the mean displacement jump may be evaluated and the closure criterion performed at each loading step.

When the closure criterion is satisfied, the layer β becomes a layer of type f (namely with closed defects at its interfaces). The contribution, $\boldsymbol{\varepsilon}^{fD}$, of closed defects to total strain of the layer is obtained using Eq. (8) at defect closure:

$$\boldsymbol{\varepsilon}^{fD} = \boldsymbol{\varepsilon}^{\beta D}(\mathbf{E}_{closure\beta}) \quad (10)$$

with $\mathbf{E}_{closure\beta}$ designating the corresponding global strain tensor. Due to the infinite friction coefficient, $\boldsymbol{\varepsilon}^{fD}$ does not evolve as long as the defects remain closed. Then, the summations involved in the definition of the damage parameters \mathbf{D} and $\bar{\mathbf{D}}$ are actualized by suppressing the layer at stake.

4. Numerical illustration

A discrete numerical solving procedure to estimate, via the MA, the local and global responses of a material under a loading generating damage has been coded in Fortran 90. As an illustration of its applicability and qualitative relevance, the results obtained in the case of successive or simultaneous discrete interfacial events (nucleation and closure of defects) occurring in a specific three-dimensional random composite are presented.

4.1. Material description and loading path

The composite studied is constituted of 400 polyhedral grains embedded in a matrix occupying 25 per cent of the total volume. Such a microstructure has been numerically generated in order to respect the requirements of the geometrical schematization (polyhedral grains, plane and parallel opposite interfaces...) and the compatibility condition briefly mentioned in Subsec. 2.2.

The morphological parameters h^α , A^α , \mathbf{n}^α and \mathbf{d}^α (see Subsec. 2.1) have been identified by simple geometrical measures for each of the 2400 layers present in the microstructure. Elastic moduli of the constituents are: $E = 120\text{GPa}$, $\nu = 0,3$ for the grains and $E = 4\text{GPa}$, $\nu = 0,45$ for the matrix. For the simulation presented in the following, the critical value, $d_{critical}$, and associated quantity λ involved in the nucleation criterion are tentatively chosen as follows: $d_{critical} = 3,548 \mu\text{m}$ and $\lambda = h/10$ where $h=0,029\text{mm}$ is the thickness of the thinnest layer in the volume. At last, the roughness of the interfaces is neglected and therefore strain-like quantities $\mathbf{r}^{\beta D}$ are taken as nulls.

The macroscopic displacement gradient \mathbf{F} (and corresponding \mathbf{E}) are the only data required by the MA to define the loading path; indeed no boundary condition has to be explicitly posed on the volume boundaries. The composite is subjected to the following loading path:

- 1/ “Tension”: incremental extension in the direction **1** ($\Delta F_{11} > 0$) whereas contractions are applied in directions **2** and **3** with $\Delta F_{22} = \Delta F_{33} = -0,3 \Delta F_{11}$.
- 2/ Simple shear: $\Delta F_{12} > 0$.
- 3/ “Compression”: incremental loading inverse to the first one: $\Delta F_{11} < 0$ and $\Delta F_{22} = \Delta F_{33} = -0,3 \Delta F_{11}$.

4.2. Homogenized stress as a function of damage local events

All the interfaces being characterized and the criteria formulated at the scale of these interfaces, the MA gives access to the position and morphology of defects within the microstructure in addition to the homogenized response. These results

allow 3D representations of the damaged microstructure. Since the nucleation has been supposed in normal mode, a defect is open before being possibly closed. In order to clearly detect the opening/closure transitions, only open defects are represented in the visualizations. When open defects are nucleated they appear and when they close they disappear. Obviously, it does not mean that closed defects are no longer present in the microstructure. Fig. 3 presents the evolution of the homogenized stress Σ_{11} with macroscopic axial strain E_{11} . For significant points ((1) to (9)) in Fig. 3, Fig. 4 presents 3D visualisations of the microstructure, showing the position and orientation of open defects, and also representations of the homogenized Young's modulus in the plane $(1,2)$, i.e. $E(\mathbf{m})$ with \mathbf{m} an arbitrary direction of the plane. These representations allow to follow the evolution of damage induced anisotropy (embodied by the tensorial parameters \mathbf{D} and $\bar{\mathbf{D}}$). Parallel setting of Figs. 3 and 4 allows the following observations:

- (1): sound material, elastic linear behaviour.
- From (2) to (4): progressive nucleation of defects (red) with normal close to $\mathbf{1}$ as expected with a nucleation criterion in normal mode considering the loading applied. The response is non linear with progressive softening. At the end of «tension», E is principally degraded in the axial direction $\mathbf{1}$.
- Between (4) and (5): the simple shear leads to the nucleation of defects (green) with normal more dispersed. These defects add to the first population. The parameters \mathbf{D} and $\bar{\mathbf{D}}$ evolve, Σ_{11} decreases whereas E_{11} is constant. At the end (5), the anisotropy is more pronounced, see the ellipsoidal form of $E(\mathbf{m})$.
- After (5), the «compression» begins. A first stage, before the truly «compression» (i.e. $E_{11} < 0$), consists in the unloading of E_{11} until $E_{11} = 0$. In the zoomed zone (green in Fig. 3) one observes the progressive closure of defects, in particular those nucleated in «tension» which are all closed in (7). This leads to the progressive recovery of E (via suppression of elements in \mathbf{D} and $\bar{\mathbf{D}}$). The recovery is complete when the (green) defects nucleated during simple shear are also closed (8). These results illustrate the ability of the MA to deal with unilateral effects. At last, one observes residual macroscopic effects (see Fig. 3) due to the distortion of closed defects (through $\{\epsilon^D\}$).
- When pursuing the «compression», defects normal to transverse directions $\mathbf{2}$ and $\mathbf{3}$ are nucleated. At the end, E is degraded in the direction $\mathbf{2}$ (see Fig. 4), but not in the axial direction since the closed defects are blocked.

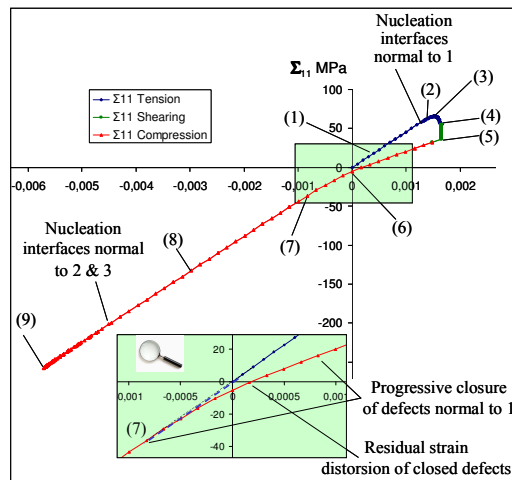


Fig.3. Homogenized Σ_{11} versus E_{11} for simulated “tension” - simple shear - “compression”.

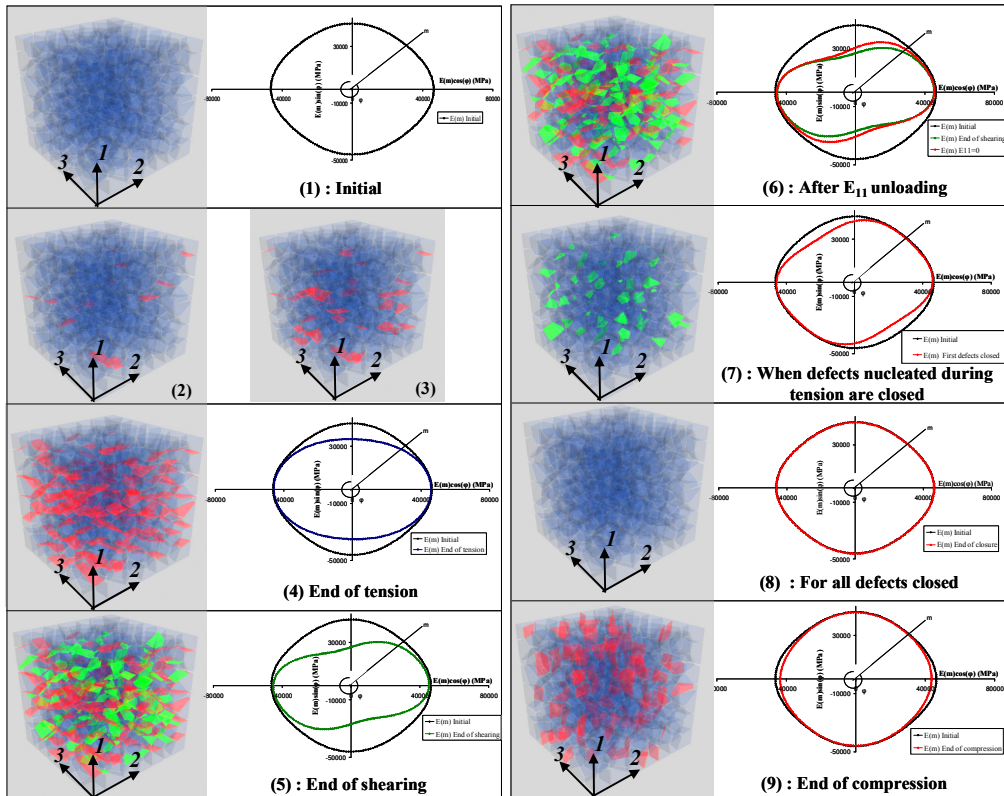


Fig.4. Position and orientation of open defects and representations of the homogenized Young's modulus.

5. References

- [1] C. Nadot-Martin, M. Touboul, A. Dragon and A. Fanget, in: O. Cazacu ed., Multiscale Modeling of Heterogeneous Materials: From Microstructure to Macro-scale Properties, ISTE/Wiley, 2008, pp. 218-237
- [2] A. Rekik, F. Auslander, M. Bornert, A. Zaoui, Int. J. Solids. Struct. 44 (2007) 3468-3486
- [3] C. Nadot-Martin, H. Trumel, A. Dragon, Eur. J. Mech. A/Solids 22 (2003) 89-106.
- [4] M. Touboul, C. Nadot, A. Dragon, A. Fanget, Arch. Mech. 59 (2007) 403-433
- [5] N. Lahellec and P. Suquet, Int. J. Solids. Struct. 44 (2007) 507-529
- [6] J. Christoffersen, J. Mech. Phys. Solids 31 (1983) 55-83
- [7] M. Touboul, PhD Thesis, 2007, University of Poitiers-ENSMA
- [8] C. Nadot, A. Dragon, H. Trumel, A. Fanget, J. Theor. Appl. Mech. 44 (2006) 553-583
- [9] H. Moulinec and P. Suquet, Eur. J. Mech. A/Solids 22 (2003) 751-770
- [10] S. Dartois, D. Halm, C. Nadot-Martin, A. Dragon and A. Fanget, Mechanics of Materials, forthcoming paper.